Proceedings of the ASME 2011 30th International Conference on Ocean, Offshore and Arctic Engineering
OMAE2011
June 19-24, 2011, Rotterdam, The Netherlands

OMAE2011-50047

PROBABILISTIC MODEL APPLICATION IN THE INTEGRATED STABILITY ANALYSIS OF OFFSHORE ON-BOTTOM PIPELINE

Bassem S. Youssef
Centre for Offshore Foundation Systems

The University of Western Australia
Perth, Western Australia, Australia

Mark J. Cassidy
Centre for Offshore Foundation Systems

The University of Western Australia
Perth, Western Australia, Australia

Yinghui Tian
Centre for Offshore Foundation Systems

The University of Western Australia
Perth, Western Australia, Australia

ABSTRACT

Offshore pipelines provide the main link between offshore oil and gas fields and hydrocarbon development onshore. Due to their economical installation, untrenched pipelines laid “on-bottom” are finding increased popularity over other types of offshore pipelines. However, the stability of untrenched pipeline design remains the subject of criticism. In many cases around the world, severe loading conditions, such as those during hurricanes, result in severe pipeline damage and disruption of oil and gas supply.

In on-bottom pipeline stability analysis, hydrodynamic loads are applied to the pipe structure. The pipe passes these loads onto the supporting soil along its length. A variety of parameters need to be defined to model this loading scenario and to reflect the complicated interaction between the hydrodynamic load, pipe structure and the supporting soil. Moreover, there are uncertainties regarding the input values of these parameters, as any difference in these parameter values will result in a considerable difference in the final pipeline stability result (though the sensitivity to any differences is not well studied).

In this study of the offshore pipeline stability, the hydrodynamic loads are estimated using Fourier analysis, which is currently the best practice in hydrodynamic modeling. The pipe-soil interaction is simulated with a force-resultant model, which is derived from a plasticity framework and is based on the results of centrifuge test calibration. The pipeline is modeled using an integrated numerical modeling tool developed by implementing the hydrodynamic load model and force-resultant model codes in the finite element package ABAQUS. Use of the integrated modeling tool allows for the coupling effect of the hydrodynamic-pipe-soil interaction to be accounted for, with the added ability to modify the applied hydrodynamic loads due to pipe movements during the analysis.

The main aims of this paper are to demonstrate methods to estimate the probability of exceeding pipeline stability and quantify the importance of the on-bottom pipeline statistical analysis and the sensitivity of the parameters included in the pipeline stability design.

After first describing the integrated model and providing an illustrative example of its use these aims are achieved by i) performing probabilistic analysis for a typical pipeline case and investigating the probability of exceeding pipeline stability under different maximum pipeline displacement values; and ii) developing a sensitivity analysis of the input parameters included in the on-bottom pipeline stability and ranking these parameters according to their sensitivity to the pipeline stability design.

INTRODUCTION

In the on-bottom pipeline stability analysis, many parameters are included to describe the conditions surrounding the pipeline. These parameters include soil parameters, pipe parameters, ocean environment and hydrodynamic modeling parameters, and site location parameters. In the deterministic analysis of the on-bottom pipeline, a single value is assigned to each parameter. However, there are uncertainties regarding the values of these input parameters. A commonly used design approach to overcome the analysis simplification and the uncertainty in the variables is to use a safety factor. However, this method has several limitations. It tends to be overly conservative for many practical situations, and it does not provide any quantification of the design reliability. The former has obvious economic implications, and the latter fails to deliver the required input for risk evaluation.

To achieve an economical design and maximize design reliability, an accurate hydrodynamic-pipe-soil calculation should be performed, and an alternative probabilistic design approached should be considered.

HYDRODYNAMIC LOAD MODEL

Environmental conditions such as waves, currents, and their direction of approach as well as water depth and seabed roughness are major factors that affect the lateral stability of an offshore pipeline that rests on the seabed. The hydrodynamic forces acting on the offshore pipeline are usually calculated for a pipe touching the seabed. No pipe movements or embedments are included. However, in practice, the pipe may experience considerable movements or embedments.

Therefore, in the present study, a hydrodynamic modeling tool (UWAHYDRO) was used to simulate the hydrodynamic loads acting on an on-bottom pipeline and to account for the effect of pipe movements or embedments that may occur during pipeline analysis. ABAQUS calls UWAHYDRO at two main stages during the pipeline simulation. The main steps during these two stages can be briefly summarized as follows:

Stage I: Beginning of pipeline analysis

Step 1- An ocean surface time series for each node along the pipeline is generated using a wave spectrum model (JONSWAP spectrum is used in the present paper), spreading function and linear wave theory. This is in the form of the superposition of a finite number of harmonic waves:

$$\eta(x,y,t)=\sum_{i=1}^{N}\sum_{j=1}^{M}a_{i,j}\cos(\phi_{i,j}) \tag{1}$$

where

$$\phi_{i,j}=K_i x\cos\theta_j+K_i y\sin\theta_j-\omega_i t+\varepsilon_{i,j} \tag{2}$$

$$a_{i,j}=\sqrt{2\,S(\omega_i)\,D(\omega_i,\theta_j)\,\Delta\theta\,\Delta\omega} \tag{3}$$

and $\Delta\omega$ and $\Delta\theta$ are angular frequency and directional increments, $D(\omega,\theta)$ the directional spreading frequency, $S(\omega)$ the wave spectrum, K the wave number, $\varepsilon_{i,j}$ the random phase, $a_{i,j}$ the amplitude of the individual wavelets, N and M the frequency and direction increments and x and y the calculation point coordinates (axis and directions are defined in Fig. 1).

Step 2- The wave velocity (U_w) and acceleration ($\dot{U}_w$) normal to the pipeline are determined using the generated ocean surface and wave theory as described by Lambrakos (1982):

$$U_w(x,y,t)=\sum_{i=1}^{N}\sum_{j=1}^{M}a_{i,j}\,\omega_i\frac{\cosh(K_i(d+z))}{\sinh(K_i d)}\cos(\phi_{i,j})\cos(\theta_j) \tag{4}$$

$$\dot{U}_w(x,y,t)=\sum_{i=1}^{N}\sum_{j=1}^{M}a_{i,j}\,\omega_i^2\frac{\cosh(K_i(d+z))}{\sinh(K_i d)}\sin(\phi_{i,j})\cos(\theta_j) \tag{5}$$

where d is the water depth and z the distance between the pipe and the still water level.

Step 3- The drag and lift forces acting on the pipeline are estimated using the Fourier analysis model proposed by Sorenson et al. (1986). The basis of the Fourier method is that any quantity that varies periodically with a certain period T can be reproduced by the superposition of a number of sine waves with periods equal to T and smaller. The general expression of the periodic quantity $F(t)$ is given by the following:

$$F(t)=a_o+\sum_{i=1}^{5}(a_i\cos(i\omega t)+b_i\sin(i\omega t)) \tag{6}$$

where $\omega=2\pi/T$ and a_i and b_i are the Fourier coefficients of the force. These have been determined from experimental measurements (Sorenson et al. 1986). The inertial force is calculated from the wave acceleration potential flow theory for a cylinder:

$$F_I=C_M\frac{\pi}{4}\rho D^2\dot{U}_w(t) \tag{7}$$

where C_M is the inertia coefficient with a value of 3.29 (Sorenson et al. 1986).

Stage II: During the pipeline analysis

Step 4- ABAQUS calls UWAHYDRO at each time increment to provide the corresponding in-line and lift forces by interpolating the pre-calculated loads based on node coordinate and time. Before these forces are applied to the pipe element, the horizontal and vertical pipe movements are used to modify the hydrodynamic loads.

When the pipe experiences vertical penetration, it becomes less exposed to flowing water. This tends to reduce the hydrodynamic loads. These hydrodynamic reductions can be obtained by multiplying the pre-calculated hydrodynamic forces with a reduction factor derived from the experiments of Sorenson et al. (1986).

The effect of the horizontal displacement on the hydrodynamic loads is different from that described above. As outlined by AGA (1988), the horizontal movement of the pipe relative to the wave is the key parameter of this hydrodynamic reduction. The inertial force on a pipeline moving horizontally in accelerating water is calculated as follows:

$$F_{I,Mov}=F_{I,Fix}-C_a\frac{\pi}{4}\rho D^2\ddot{x}_P \tag{8}$$

where $\ddot{x}_P$ is the pipe acceleration in the horizontal direction and C_a is the coefficient of added mass. The drag and lift force for a moving pipeline are estimated as follows:

$$F_{D,Mov} = F_{D,Fix} - \frac{1}{2}\rho DC_{D,Corr}(U_e|U_e| - (U_{ep})|U_{ep}|) \quad (9)$$

$$F_{L,Mov} = F_{L,Fix} - \frac{1}{2}\rho DC_{L,Corr}(2U_e\dot{x}_P - \dot{x}_P^2) \quad (10)$$

where $\dot{x}_P$ is the pipe velocity, U_e the effective near pipe water velocity and $U_{ep} = U_e - \dot{x}_P$. The effective near pipe can be estimated as follows:

$$U_e = \left(\frac{F_{D,Fix}}{0.5\rho D}\right)^{0.5} \frac{|F_{D,Fix}|}{F_{D,Fix}} \quad (11)$$

The values of the coefficients $C_{D,Corr}$ and $C_{L,Corr}$ in Equations 9 and 10 are recommended by AGA (1988). For more details about load reductions, reference should be made to Sorenson et al. (1986), AGA (1988), Jacobsen et al. (1989) and Verley and Reed (1989). Implementation of the Fourier method within UWAHYDRO has been verified by comparing the experimental measurements of Sorenson et al. (1986) with the numerical simulation results of UWAHYDRO (Youssef et al. 2009).

PIPE-SOIL INTERACTION MODEL

Accurate modeling of pipe-soil interactions is one of the major challenges in ensuring the on-bottom stability of unburied pipelines. The use of macro-element (or alternatively force-resultant) models in pipeline analysis offers the advantages of numerical efficiency and direct incorporation into structural finite element programs.

Based on the plasticity theory, force-resultant models directly encapsulate the behavior of the pipe the underlying soil by expressing it purely in terms of the loads and the corresponding displacements. Sign convention of vertical and horizontal loads (V, H) and their corresponding displacements (w, u) as well as, the pipeline axes are defined in Fig. 1. When these models were attached as pipe-soil interaction elements in a structural finite element analysis, they proved to be a practical and effective way to describe the load-displacement behavior of a segment of pipeline (Tian and Cassidy 2008a; 2008b).

These models were introduced by Zhang (2001) and Zhang et al. (2002a; 2002b) and calibrated using centrifuge experiments of a prototypical pipe element measuring 1 m in diameter and 8 m in length. The models represent fully drained conditions. In an updated version of Tian and Cassidy (2008b) they were named UWAPIPE and consist of three models of increasing sophistication.

Only the two surface kinematic hardening model will be considered in the present paper and will be discussed further. This model is colloquially named the “bubble” model due to what appears to be an inner bubble floating within the outer surface in a simplified schematic of the model (Fig. 2). A brief description of the model’s governing equations will be presented in the following section.

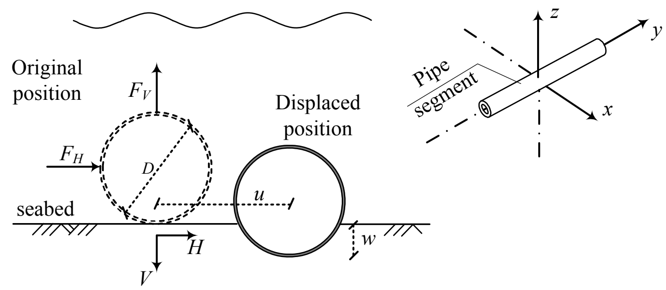

FIG. 1. LOADS AND DISPACEMENTS SIGN CONVENTION AND PIPELINE AXES

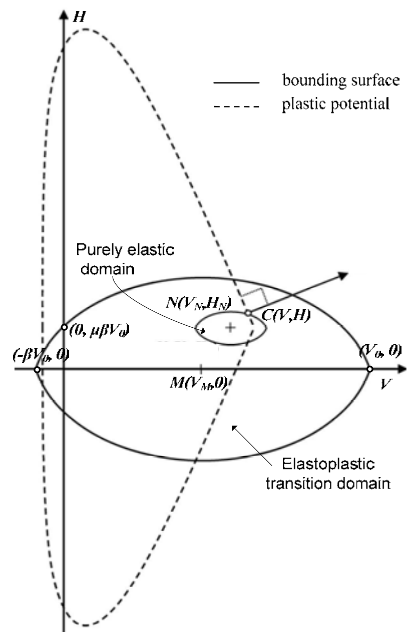

FIG. 2. THE CONCEPT OF THE YIELD AND PLASTIC POTENTIAL SURFACES

Bounding Surface and Bubble Surface

They are defined directly in terms of the load in the model as follows:

$$F = |H| - \mu\left(\frac{V}{V_0} + \beta\right)(V_0 - V) = 0 \quad (12)$$

$$f = |H - H_N| - \mu\left(\frac{V - V_N}{rV_0} + \frac{1+\beta}{2}\right)\left(\frac{1+\beta}{2}rV_0 - (V - V_N)\right) = 0 \quad (13)$$

where $F = 0$ is the outer bounding surface, $f = 0$ is the inner bubble surface, μ and β aspect ratios defining the surface shape, V_0 the size of the bounding surface representing the bearing capacity of the pipe under vertical load at the current embedment, the subscript N denotes the bubble center and r the size ratio of the bubble to the bounding surface.

Hardening Law

Hardening of the surfaces occurs by (i) isotropic hardening of the outer bounding surface and (ii) kinematic hardening of the inner bubble surface. The former is directly correlated to the vertical plastic displacement increment Δw^p as a change in surface size:

$$\Delta V_0 = \frac{k_{ve} k_{vp}}{k_{ve} - k_{vp}} \Delta w^p \tag{14}$$

$$\Delta \mu = \frac{\kappa}{D} \Delta w^p \tag{15}$$

where k_{ve} and k_{vp} are the elastic and plastic vertical stiffness, respectively, the superscript p denotes a plastic component, κ the slope of μ to w^p and D the pipe diameter. Kinematic hardening of the bubble surface is determined by the following expression:

$$\Delta \mathbf{F}_N = \Delta \mathbf{F}_M + \left(\frac{\Delta V_0}{V_0} + \frac{\Delta \mu}{\mu} \right) \frac{1-r}{r} \left(\mathbf{F} - \mathbf{F}_N \right) + \Delta \Lambda \left(\mathbf{F}_C - \mathbf{F} \right) \tag{16}$$

where the subscripts M, N and C represent the bounding surface center, bubble center and the conjugate point of the current force, respectively. $\mathbf{F} = (V, H)^T$ is the force vector. The scalar $\Delta\Lambda$ can either be explicitly evaluated according to the consistency condition of the bubble surface or implicitly iterated to integrate the constitutive equations. The bubble surface translates smoothly inside but never intersects or lies outside the bounding surface.

Flow Rule

The flow rule is formulated such that the plastic potential surface maintains a similar shape and position with the bubble surface, as shown in Fig. 2:

$$g = \left| H - H_N \right| - \mu_t \left(\frac{V}{V_0} + \beta \right)^m \left(V_0 - V \right) = 0 \tag{17}$$

where μ_t and m are the aspect ratios that control the shape of the plastic potential surface.

Elasticity

For increments inside the bubble surface, the elastic relationship of the model is defined as:

$$\Delta \mathbf{F} = \begin{Bmatrix} \Delta V \\ \Delta H \end{Bmatrix} = \mathbf{D}^e \Delta \mathbf{U}^e = \begin{bmatrix} k_{ve} & 0 \\ 0 & k_{he} \end{bmatrix} \begin{Bmatrix} \Delta w^e \\ \Delta u^e \end{Bmatrix} \tag{18}$$

where $\mathbf{U}=(w, u)^T$ is the displacement vectors, k_{he} the horizontal elastic stiffness, Δ represents an increment and the superscript e denotes an elastic component.

INTEGRATED NUMERICAL MODELING

The hydrodynamic load model (UWAHYDRO) and the pipe-soil model (UWAPIPE) are written in FORTRAN90 and attached to the ABAQUS through the user subroutines DLOAD and UEL respectively. The simulation components are as shown in Fig. 3. The pipeline structure is modeled as a beam element in ABAQUS with the hydrodynamic load modeled as distributed load acting on the beam elements using UWAHYDRO. The pipe-soil interaction is modeled as a macro-element attached to each pipe segment node; using numerous UWAPIPEs. The integrated ABAQUS program follows the following procedure:

1- At the start of the analysis, ABAQUS calls the DLOAD subroutine to generate the hydrodynamic loads along the pipeline (*Stage I*). The hydrodynamic loads of a stationary unburied pipe are then developed.

2- At each time increment, ABAQUS calls the user subroutine DLOAD to provide the modified hydrodynamic loads to the corresponding pipeline segment (*Stage II*).

3- The UWAPIPE model is called through the UEL subroutine. The incremental displacements of the current node is used to update the mode state variables and the stiffness matrix is fed back to ABAQUS.

4- ABAQUS assemblies the global stiffness matrix and solve the incremental displacement.

5- ABAQUS uses a Newton-Raphson iteration scheme for steps 3 and 4 until convergence is reached.

Only steps 2 to 5 are repeated with each time increment until the end of the pipeline simulation time.

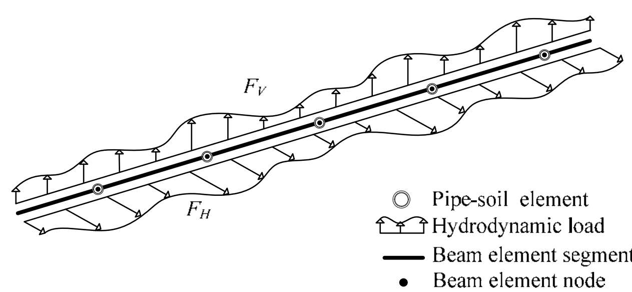

FIG. 3. PIPELINE MODEL COMPONENTS

ILLUSTRATIVE EXAMPLE

An example of long pipeline analysis will be discussed to present the framework of the developed integrated modeling program. The simulated pipeline is assumed to be straight, 1250 m in length and laid directly on a flat sea bed at a water depth of 55 m. The pipeline is divided into 250 pipe elements, each 5 m in length. This requires a UWAPIPE element at each structural node (251 UWAPIPE elements), as shown in the pipeline details (Fig. 4). The pipeline was subjected to one hour of storm loading. The modeling input parameters are provided in Table 1.

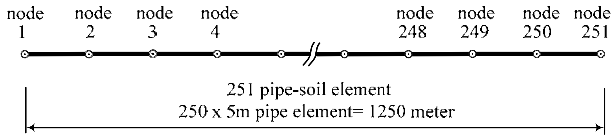

FIG. 4. PIPELINE DETAILS

At the beginning of the analysis, ABAQUS calls UWAHYDRO to generate the hydrodynamic loads for all of the pipeline nodes. These horizontal and vertical loads acting at an arbitrary node (node number 38) are presented in Fig. 5. However, these loads are different at each node due to the directional spreading function used by UWAHYDRO. Loads acting on the longitudinal section along the pipeline at an arbitrary time of 2580 s (43 minutes) are shown in Fig. 6.

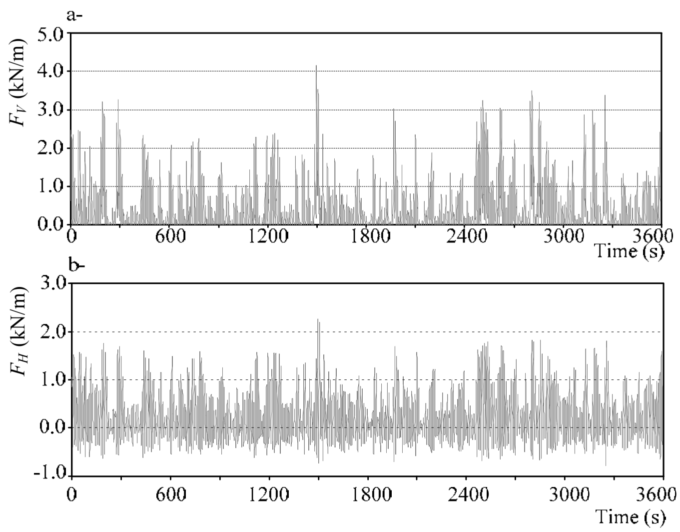

FIG. 5. HYDRODYNAMIC LOADS (NODE NUMBER 38)

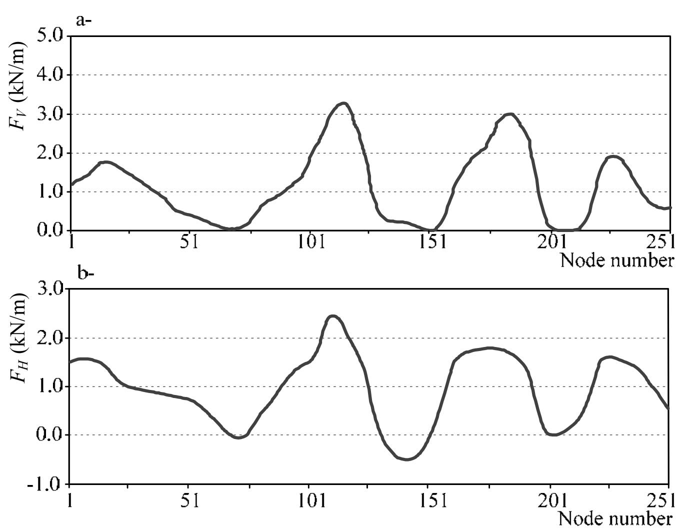

FIG. 6. HYDRODYNAMIC LOADS (TIME 2580 s)

The horizontal and vertical pipeline displacements after a certain analysis time are presented in Fig. 7. Again, the displacements history is different from one node to another, tracing the displacements of one the pipeline nodes (node number 38) is provided in Fig. 8.

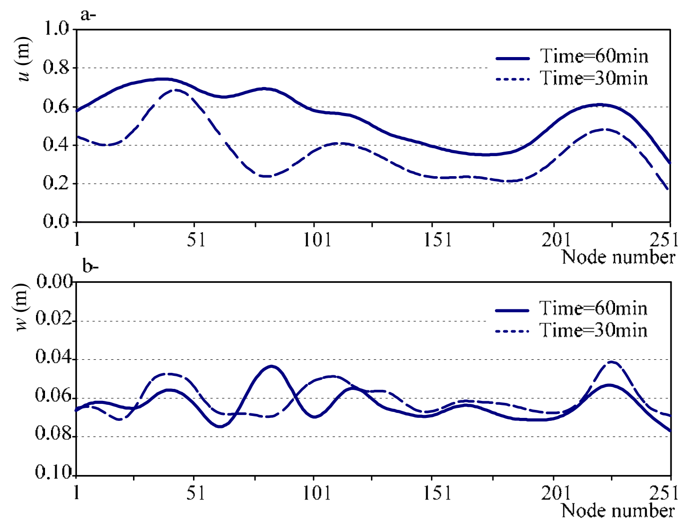

FIG. 7. PIPELINE DISPLACEMENTS (TIME)

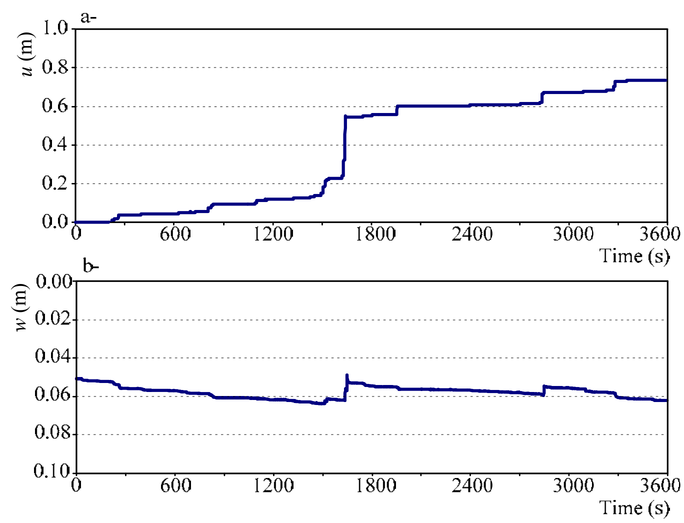

FIG. 8. PIPELINE DISPLACEMENTS (NODE NUMBER 38)

UNCERTAINTIES IN THE ANALYSIS

To quantify the uncertainty in the on-bottom pipeline analysis, it is necessary to define the modeling variables that govern the pipeline stability analysis. These are known as the set of basic random variables and their statistical distribution estimated. The set determined as significant in the examples of this paper are detailed in Table 2. This section will discuss why these were chosen and how their mean values and variability estimated. The illustrative examples are most relevant to the Australian North West Shelf region. The basic random variables in Table 2 are divided into three categories, namely the soil modeling parameters, pipe modeling parameters and the hydrodynamic modeling parameters.

Soil Modeling Parameters

The mean values of the UWAPIPE parameters were best-fit from centrifuge experiment calibrations. However, there was scatter within the data and this is accounted for in determining parametric distributions.

Plastic Vertical Stiffness (k_{vp}). The plastic vertical loading stiffness was estimated from the linear portion of the vertical load displacement curves of the physical modeling. Using the test results presented by Zhang (2001) on typical calcareous sand found in the Australian North West Shelf region, an average value of plastic vertical loading stiffness of 363 kN/m was calculated over 36 centrifuge tests with a standard deviation of 105 kN/m. The value of 400 kN/m recommended by Zhang (2001) was most probably based on calibration of a sub-set of the tests. Adding to this database are the tests of Tian et al. (2010a), with 40 test results using the same soil type having a mean plastic vertical loading stiffness of 375 kN/m and a standard deviation of 92 kN/m. The original 400 kN/m value with a CoV of 25% has been assumed in this paper.

Yield Surface Shape Parameter (μ_o) and Its Gradient with Depth (κ). These values were derived from 11 normal-loaded sideswipe tests presented by Zhang (2001) and 10 tests presented by Tian et al. (2010a). Eleven values of plastic vertical displacement and their corresponding μ_o presented by Zhang (2001) were used in a linear regression equation to produce a mean value of 0.44 with a standard deviation of 0.06 for μ_o and a mean value of 0.46 with a standard deviation value of 0.21 for κ. Meanwhile, using the 10 sideswipe tests results presented by Tian et al. (2010a) yielded a mean value of 0.57 with a standard deviation of 0.02 for μ_o and a mean value of 0.06 and a standard deviation of 0.09 for κ.

Pipe Modeling Parameters

Pipeline Geometry. Several pipe properties are used in the pipeline stability analysis, including the cross-sectional area, moment of inertia and Young's modulus. In offshore fields, where pipelines are employed over several kilometers in length, there is possibility that these properties could change either during construction, installation or operation for many reasons. Among these is the pipeline manufacturing tolerance of both the pipe wall thickness and pipe diameter can result in a change in the cross-sectional area and moment of inertia. Moreover, during the laying of the pipeline, the pipe may experience excessive bending moments and internal stresses, especially in the sagbend zone. This results in a change in pipe geometry (Igland and Moan 2000; Brown et al. 2004).

In addition, marine growth may occur on the pipeline and result in the addition of extra hydrodynamic loads, causing the pipeline to assume a larger circumferential area and increased surface roughness (Ralph and Troake 1980; Wolfram and Theophanatos 1990; Mbadinga et al. 2007; NORSOK standard 2007). A CoV value of 10% was chosen to reflect the possible changes in the *EI* value.

Load Concentration during the Pipeline Laying. Extensive research work has discussed the phenomenon of pipeline penetration during the laying process due to force concentration in the touchdown zone (Cathie et al. 2005; Randolph and White 2008; Westgate et al. 2010). A value of 2.0 and 4.2 times the pipe self-weight was suggested by Cathie et al. (2005) for the case of weak soil and strong soil, respectively. However, the observations and numerical simulation results of Westgate et al. (2010) outlined that many variables can affect this force concentration value; among these are the sea state during the pipeline laying, water depth, wind speed and direction and laying vessel speed. There is, however, considerable uncertainty to what value to be applied in a numerical simulation, with a relatively high CoV of 25% therefore used.

Hydrodynamic Modeling Parameters

Water Depth. The water depth defined in the pipeline analysis can vary due to several reasons, such as the tide effect, the accuracy of devices that measure water depth, the measuring platform movement or seabed irregularity (though a small CoV is assumed). The Australian North West Shelf tide is semi-diurnal with a maximum height of 10 meters (Cresswell and Badcock 2000).

Spectral Properties H_s and T_p. The significant wave height, H_s, and the peak wave period, T_p, are the key parameters in generating the ocean surface. The hydrodynamic forces acting on the on-bottom pipeline depends, to a great extent, on the ocean surface generated. McConochie et al. (2010) outlined the variation of the peak wave period and significant wave height as historical measurements in the NWS region.

Current Velocity and Direction. The current is an important parameter in calculating the hydrodynamic loads in the pipeline stability analysis. Current has two components: a cross-shore component and a long-shore component. The magnitudes of both components magnitude vary along the Australian North West Shelf region throughout the year (Holloway and Nye 1985; Fandry and Steedman 1989).

Hydrodynamic Forces Coefficients. The coefficients used to drive the hydrodynamic forces, either the Morison equation coefficients or Fourier analysis model coefficients, have certain accuracy in representing the forces correctly. Moreover, these coefficients are based on physical modeling tests within a certain range of Keulegan-Carpenter numbers and current-to-wave velocity ratios. This test data has significant scatter and best estimates of CoV are provided in Table 2

Pipeline Roughness. Pipeline roughness has a significant effect on the estimated hydrodynamic forces acting on the pipeline (Sorenson et al. 1986). During operation, the pipe roughness will change due to marine growth on the exposed pipe surface.

Different marine growth thicknesses are suggested to be considered in the analysis. This is based on site conditions like water depth, sea bed formation, average water temperature and structure employment age (Ralph and Troake 1980; Wolfram and Theophanatos 1990; Damgaard and Palmer 2001; Mbadinga et al. 2007; NORSOK standard 2007).

RELIABILITY OF ON-BOTTOM PIPELINE STABILITY

The reliability of on-bottom pipeline stability is defined as the probability that pipe displacement will not exceed the maximum displacement value determined by the designer. Reliability is equal to the probability of failure subtracted from unity. In this case, failure is defined as the exceeding of the displacement limit state. From basic structural reliability theory, the failure probability is defined as

$$P_f = P\left[G(X) \le 0\right] = \int_{G(X)\le 0} f_X(X)dx \tag{19}$$

where $G(X)$ is the failure function, X is a set of k random basic variables (Table 2) and $f_X(X)$ is the multi-variant density function of X. Three possible values of the failure function are the failure state $G(X) < 0$, critical state $G(X) = 0$ or safe state $G(X) > 0$.

Failure criteria are usually set on the limiting factors of strength or behavior of the structure:

$$G(X) = R - S \tag{20}$$

where R is the resistance (or the maximum allowed pipeline displacement) and S is the serviceability (in this case, the maximum horizontal pipeline displacement experienced during the analysis).

RELIABILITY CALCULATION TECHNIQUES

The evaluation of pipeline displacement design reliability is of extreme importance in pipeline analysis, especially when the variables included in the analysis are random. It is necessary to quantify and identify the significance of each of these variables in the pipeline displacement analysis.

As mentioned above, the reliability of the pipeline displacement estimation is based on the integral of Equation 19. The Monte Carlo simulation method is one of the most widely accepted methods in calculating this integral. For each simulated vector of random variables X, a complete numerical analysis must be performed to estimate the maximum horizontal pipeline displacement.

To achieve these calculations with reasonable accuracy, a considerable number of simulation cases must be carried out. For a long pipeline in an hour storm this has a prohibitive computational cost (this represents why such analysis type is not regularly performed). An alternative method is introduced here. A Response Surface model is used to substitute the Monte Carlo process. Only a smaller number of integrated pipe on-bottom stability simulation cases are required to calibrate the response surface. Once the response surface model is developed, its polynomial will replace the ABAQUS simulation to predict the resulting displacement response, providing a significant computational saving. Moreover, the response surface polynomial can be used in carrying out the statistical analyses for the pipeline stability, such as determining the probability of exceedance, or measuring variable sensitivity.

RESPONSE SURFACE METHOD

The horizontal pipeline displacement depends on many variables and can be expressed as a function of these variables:

$$\eta = g(X_1, X_2, X_3, \ldots, X_k) \tag{21}$$

where X_i is the set of basic random variables. In general, η is described only implicitly. In the response surface method, the original implicit form is replaced by an approximate explicit function written directly in terms of basic random variables. In this paper, a second-order response surface function with mixed terms is used to model the maximum horizontal pipeline displacement:

$$\hat{S}(X) = a + \sum_{i=1}^{k} b_i X_i + \sum_{i=1}^{k} c_i X_i^2 + \sum_{j=1}^{k}\sum_{i<j}^{k} d_{ij} X_i X_j + \varepsilon \tag{22}$$

where X_i and X_j are the ith and jth components, respectively, of the set of random variables, a, b_i, c_i and d_{ij} the free parameters requiring evaluation (a total of $1 + 2k + k(k-1)/2$ distinct design points) and ε the error of fit. The term $\hat{S}$ represents the service response predicted by the Response Surface. This form was chosen for its ability to model the response with significant system curvature.

There are many Response Surface designs. In this study, the most popular class of second-order designs Center Composite Design (CCD) was used (Myers and Montgomery 1995; Box and Wilson 1951). Much of the motivation for using the CCD derives from its use in sequential experimentation. It involves the use of a two-level factorial combined with the axial or star points and the center point. As a result, the design involves (2^k) factorial points, ($2k$) axial points and (cp) central points. Fig. 9 shows the CCD for $k = 2$

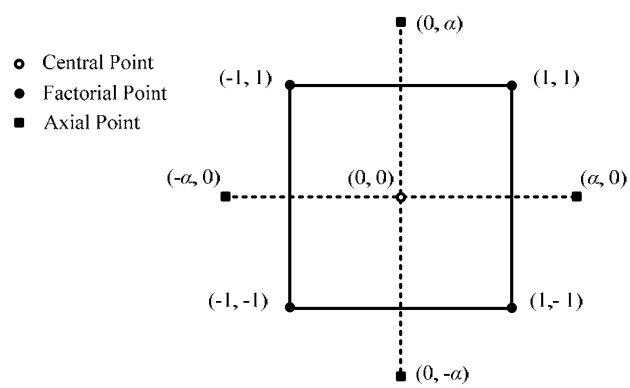

FIG. 9. CCD FOR CASE *k*=2

The factorial points represent a variance in optimal design for a first-order model or a first-order plus two-factor interaction model. The factorial points are the only points that contribute to the estimation of the interaction terms. The axial points contribute to the estimation of the quadratic terms, while the center points are mainly important to the estimation of the pure error. The central composite design resides in the flexible selection of the axial distance, α, and the number of the central points, cp. The axial points are selected to be located at ($\mu \pm h\sigma$), where μ and σ are the mean and the standard deviations of the random variables X, and h is an arbitrary factor. The values of h varies from (1.0 to $\sqrt{k}$), the former placing all the axial points on the face of a cube or hypercube and the latter resulting in all points being placed on a common sphere (Myers and Montgomery 1995).

DEVELOPING THE RESPONSE SURFACE

Eight basic random variables were selected to develop the response surface for the maximum horizontal pipeline displacement. The mean values and standard deviations of the eight variables are shown in Table 2. Despite the fact that the response equation developed using eight parameters has 45 unknowns, a total number of 273 numerical simulation cases were used to generate the polynomial (Factorial points $2k$ =256 cases, Axial points $2k$ =16 cases plus one central point).

The 273 simulation cases were carried out using the integrated pipeline analysis program presented. It should be noted that, for all the response surface cases, the same random seed was used to develop the ocean surface. Therefore, *stage I,* the hydrodynamic loads for the pipe invert at the seabed are consistent for all analysis.

It is acknowledged that there will also be significant variability due to the inherent random nature of the storm, and quantifying this is an area of ongoing research interest. However, in selecting the random seed for these analyses, 100 cases with 100 different random seeds were analyzed using the parameters mean values listed in Table 2. The random seed corresponding to the average horizontal displacement case was then used for the response surface points reported in this paper.

Moreover, because the central point case assumes all of the mean values, it is the previous illustrative example with an average displacement of 0.55 m with maximum and minimum displacements of 0.72 m and 0.34 m, respectively.

Determination of Polynomial Unknowns and Accuracy of Response Surface

The polynomial unknowns in the response surface equation are evaluated by a least-squared estimation method. Though further details will not be provided here, the resulting polynomial coefficients of the response surface are listed in Table 3. An examination of the response surface showed that it provides an adequate estimation to the numerical simulation. This was confirmed numerically through the methodology of prediction error sum of squares (PRESS) method proposed by Allen (1974), however, again details of this method are too convoluted for the space available in this paper. A visual inspection is provided in Fig. 10, where the maximum displacement predicted by the response surface method is plot against the numerical result from ABAQUS for both the 273 numerical cases originally used in developing the response surface and another 125 sets of normally distributed random variables. As can be seen in the Fig. 10 the accuracy is good.

PROBABILITY OF EXCEEDANCE CALCULATION

The probability of exceedance forecasts the probability that the maximum horizontal pipeline displacement will exceed a certain value.

A Monte Carlo simulation of 10000 different cases were calculated using the response surface polynomial to determine the probability of exceedance of the maximum pipeline stability design. Eight independent sets of 10000 normally distributed random numbers were assigned to the eight response surface polynomial parameters to calculate the pipe displacement.

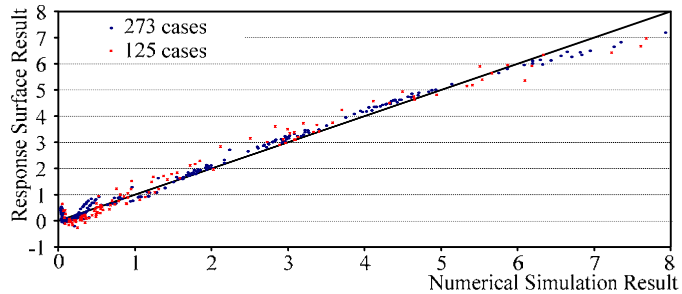

FIG. 10. COMPARING NUMERICAL SIMULATION AND RESPONSE SURFACE POLYNOMIAL RESULTS

The analysis results for the 10000 cases yielded a mean value of 1.76 m with a standard deviation of 2.37 m, with a 50% probability of exceedance value of 0.89 m. As expected, the 50% exceedance value is close to the maximum horizontal pipeline displacement 0.72 m calculated by numerical simulation, when all random variables equal their mean values. Using the results presented in Fig. 11, the probability of failure for a certain value of maximum horizontal pipeline displacement can be easily determined. For instance, the probability of failure calculated over four proposed maximum pipeline displacement 1, 2.5, 5 and 10 times the pipe diameter are 0.476, 0.248, 0.092 and 0.014, respectively.

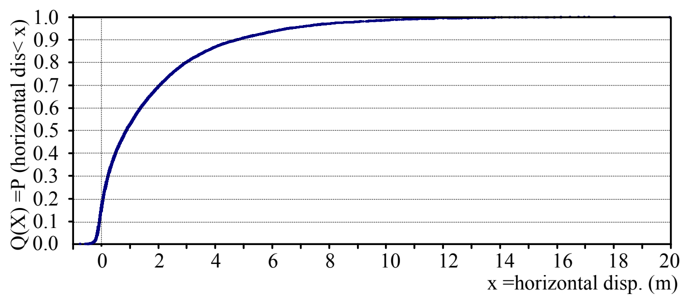

FIG.11. MONTE CARLO SIMULATION (PROBABILITY OF EXCEEDANCE) USING 10000 CASES

It is remarkable from the result that the distribution has a long tail of high displacements at low probabilities. As shown in Fig. 11, only 1.5% of the results only are plotted within a horizontal displacement range between 10 and 20 m. Moreover, almost 18% of the horizontal displacements are negative values, reflecting a feature of inaccuracy at low values in the proposed response surface. This was not considered important as any displacement values near zero indicate a stable pipeline (and these negative values could just be assumed as zero).

SENSITIVITIES OF THE BASIC RANDOM VARIABLES

Because all input random variables do not have equal influence on the pipeline analysis, it is desirable to identify the importance of each random variable included in the response surface. A sensitivity study was carried out by Monte Carlo simulation using the developed maximum horizontal pipeline displacement response surface polynomial, where a measure called the sensitivity index was used to quantify the influence of each basic random variable. The relative importance of the random variable X_i was calculated as $\partial P_f / \partial \mu_{Xi}$ (Karunakaran 1993; Cassidy 1999). Within the Monte Carlo calculation, this sensitivity measure denoted $S_{\mu Xi}$ was defined as

$$S_{\mu Xi} = \frac{P_f(\mu_X + d\mu_{Xi}) - P_f(\mu_X)}{d\mu_{Xi} - \mu_{Xi}} \qquad (23)$$

where $d\mu_{Xi}$ is a small change in the mean value of the random variable X_i. In this study, this small change was assumed to be a 1% (increase or decrease, depending on which change enlarged the response).

A total of 80000 cases were investigated using the developed response surface polynomial, 10000 cases for each individual variable. After placing the results in descending order, the probability of failure and sensitivity index were calculated over the eight sets for maximum horizontal displacements of 1.0, 2.5, 5.0 and 10.0 times the pipe diameter. The results of these analyses are listed in Table 4. The influence of the basic random variables on pipe displacement is therefore shown, with the variables ranked in order of importance. The following can be concluded:

-The water depth ranked as the most significant variable among the variables listed, even though it has the lowest variability at only 3.5%. This result agrees with the finding of Youssef et al. (2010), who reported that the water depth significantly affects the final horizontal pipeline displacement.

-Fourier drag and lift forces coefficients ranked second among the eight parameters across the four levels of maximum horizontal pipeline displacement. This is also expected because the lift force is the main factor that lifts the pipeline from the seabed and enables the pipeline to be easily moved laterally under the action of the drag and inertial forces.

-In the third and fourth levels, the yield surface parameter and the plastic vertical stiffness parameters were, respectively, the most significant. These two parameters have a direct effect in determining the horizontal and vertical forces that the pipeline can resist at any time.

-V_0 is the least important parameter in the list, which agrees with the finding of Tian et al. (2010b). In the intensive analysis carried out to investigate the effect of increasing the Load Concentration Factor (LCF), or the factor V_0 in this paper, on the final pipeline displacement, the analysis considered various LCF values starting from 2 times the pipe self-weight up to 20 times the self-weight in increments of 2 times the pipe self-weight. The result shows that increasing the LCF up to 10 times the pipe self-weight has almost no considerable effect on the final pipeline lateral displacement.

CONCLUSION

An integrated pipeline stability analysis model is introduced with an illustrative example of its use. Reliability analysis of on-bottom pipeline stability was performed using Monte Carlo simulation. The computational expense required to perform Monte Carlo simulation of complex pipeline analysis is overcome by developing a response surface polynomial to replace the traditional numerical simulation procedure described. This response surface was shown to be efficient in determining the probability of exceedance of the maximum pipeline displacement and the sensitivity of the stability analysis input parameters.

The sensitivity study of the input parameters revealed that the water depth is the most sensitive parameter in the parameters list, and the load concentration factor at the touchdown zone V_0 is among the least significant parameters in the pipeline stability design parameters list. The sensitivity results provide guidance to engineers as to what uncertainties should be reduced before a pipe is designed.

It should be noted that the probability of exceedance and sensitivity study results correspond to the parameter values and pipeline design conditions presented in this paper.

ACKNOWLEDGMENTS

This research was undertaken within the CSIRO Wealth from Oceans Flagship Cluster on Subsea Pipelines with funding from the CSIRO Flagship Collaboration Fund. The first author appreciates the support from Society for Underwater Technology through his SUT 2011 educational support fund. The second author is the recipient of an Australian Research Council Future Fellowship.

REFERENCES

[1] AGA (1988). "Submarine Pipeline On-Bottom Stability." Report on projects PR-178-516 & PR-178-717, Prepared by Brown & Root, Houston, Texas, USA.

[2] Allen, D. M. (1974). "The Relationship between Variable Selection and Data Agumentation and a Method for Prediction." *Technometrics*, 16(1).

[3] Box, G. E. P., and Wilson, K. B. (1951). "On the Experimental Attainment of Optimum Conditions." *Journal of the Royal Statistical Society. Series B (Methodological)*, 13(1), 1-45.

[4] Brown, G., Tkaczyk, T., and Howard, B. (2004). "Reliability Based Assessment of Minimum Reelable Wall Thickness for Reeling." *ASME Conference Proceedings*, 2004(41766), 1951-1960.

[5] Cassidy, M. J. (1999). "Non-Linear Analysis of Jack-Up Structures Subjected to Random Waves." Thesis(Ph.D), New College, Oxford, UK.

[6] Cathie, D. N., Jaeck, C., Ballard, J. C., and Wintgens, J. F. (2005). "Pipeline geotechnics – state-of-the-art." *Proc. of the Int. Symp. on the Frontiers in Offshore Geotechnics: ISFOG 2005*, Taylor and Francis Group, Perth, Australia, pp 95-114.
[7] Cresswell, G. R., and Badcock, K. A. (2000). "Tidal mixing near the Kimberley coast of NW Australia." *Marine and Freshwater Research*, 51(7), 641-646.
[8] Damgaard, J. S., and Palmer, A. C. (2001). "Pipeline stability on a mobile and liquefied seabed: a discussion of magnitudes and engineering implications." *proc. 20th International Conference on Offshore Mechanics and Arctic Engineering,* Rio de Janeiro, Brazil.
[9] Fandry, C., and Steedman, R. (1989). "An investigation of tropical cyclone-generated circulation on the North-West Shelf of Australia using a three-dimensional model." *Ocean Dynamics*, 42(3), 307-341.
[10] Holloway, P. E., and Nye, H. C. (1985). "Leeuwin current and wind distributions on the southern part of the Australian North West Shelf between January 1982 and July 1983." *Marine and Freshwater Research*, 36(2).
[11] Igland, R. T., and Moan, T. (2000). "Reliability Analysis of Pipelines During Laying, Considering Ultimate Strength Under Combined Loads." *Journal of Offshore Mechanics and Arctic Engineering*, 122(1), 40-46.
[12] Jacobsen, V., Bryndum, M. B., and Bonde, C. (1989). "Fluid Loads on Pipelines: Sheltered or Sliding." *Proc. 21st Offshore Technology Conference,* Houston, Texas, USA.
[13] Karunakaran, D. (1993). "Nonlinear dynamic response and reliability analysis of drag-dominated offshore structures." Thesis(Ph.D), NTH, Norway.
[14] Lambrakos, K. F. (1982). "Marine pipeline dynamic response to waves from directional wave spectra." *Journal of Ocean Engineering*, 9(4), 385-405.
[15] Mbadinga, M. L. B., Schoefs, F., Quiniou-Ramus, V., Birades, M., and Garretta , R. (2007). "Marine Growth Colonization Process in Guinea Gulf: Data Analysis." *Journal of Offshore Mechanics and Arctic Engineering*, 129(2), 97-106.
[16] Mcconochie, J. D., Stroud, S. A., and Mason, L. B. (2010). "Extreme Hurricane Design Criteria for LNG Developments: Experience Using a Long Synthetic Database." *Offshore Technology Conference,* Houston, Texas, USA.
[17] Myers, R. H., and Montgomery, D. C. (1995). *Response surface methodology: Process and product optimization using designed experiments*, John Wiley & Sons, New York.
[18] Norsok Standard (2007). "Actions and action effects." Standards Norway, N-003, Edition 2.
[19] Ralph, R., and Troake, R. P. (1980). "Marine Growth on North Sea Oil and Gas Platforms." *Offshore Technology Conference,* Houston, Texas.
[20] Randolph, M. F., and White, D. J. (2008). "Pipeline Embedment in Deep Water: Processes and Quantitative Assessment." *Offshore Technology Conference,* Houston, Texas, USA.
[21] Sorenson, T., Bryndum, M., and Jacobsen, V. (1986). "Hydrodynamic Forces on Pipelines- Model Tests." Danish hydraulic Institute (DHI), Contract PR-170-185. Pipeline Research Council International Catalog No. L51522e.
[22] Tian, Y., and Cassidy, M. J. (2008a). "A Practical Approach to Numerical Modeling of Pipe-Soil Interaction." *Proc. 18th International Offshore (Ocean) and Polar Engineering Conference,* Vancouver, BC, Canada.
[23] Tian, Y., and Cassidy, M. J. (2008b). "Modelling of Pipe-Soil Interaction and Its Application in Numerical Simulation." *The International Journal of Geomechanics*, 8(4), 213-229.
[24] Tian, Y., Cassidy, M. J., and Gaudin, C. (2010a). "Advancing pipe-soil interaction models in calcareous sand." *Applied Ocean Research*, 32(3), 284-297.
[25] Tian, Y., Cassidy, M. J., and Youssef, B. S. (2010b). "Consideration for on-bottom stability of unburied pipelines using force-resultant models." *Proc. 20th International Offshore (Ocean) and Polar Engineering Conference,* Beijing, China.
[26] Verley, R. L. P., and Reed, K. (1989). "Use of laboratory force data in pipeline response simulations." *Proc. International Offshore Mechanics and Arctic Engineering Symposium,* New York, pp 157-165.
[27] Westgate, Z. J., Randolph, M. F., White, D. J., and Li, S. (2010). "The influence of sea state on as-laid pipeline embedment: A case study." *Applied Ocean Research*, 32(3), 321-331.
[28] Wolfram, J., and Theophanatos, A. (1990). "Marine Roughness And Fluid Loading." *Environmental Forces on Offshore Structures and Their Predictions: Proceedings of an international conference,* London, UK.
[29] Youssef, B. S., Cassidy, M. J., and Tian, Y. (2009). "Numerical Modelling of Hydrodynamic Forces." *Research Report No. C:*2520, Centre for Offshore Foundation System, University of Western Australia, Perth.
[30] Youssef, B. S., Cassidy, M. J., and Tian, Y. (2010). "Balanced Three-Dimensional Modelling of the Fluid-Structure-Soil Interaction of an Untrenched Pipeline." *Proc. 20th International Offshore (Ocean) and Polar Engineering Conference,* Beijing, China.
[31] Zhang, J. (2001). "Geotechnical stability of offshore pipelines in calcareous sand." Thesis (Ph.D.), University of Western Australia.
[32] Zhang, J., Stewart, D. P., and Randolph, M. F. (2002a). "Kinematic Hardening Model for Pipeline-Soil Interaction under Various Loading Conditions." *The International Journal of Geomechanics*, 2(4), 419-446.
[33] Zhang, J., Stewart, D. P., and Randolph, M. F. (2002b). "Modelling of shallowly embedded offshore pipelines in calcareous sand." *Journal of Geotechnical and Geoenvironmental Engineering ASCE*, 128(5), 363-371.

TABLE 1. PROPERTIES USED IN THE EXAMPLES

Category	Symbol	Value	Description
UWAHYDRO	H_s	12 m	Significant wave height
	T_p	10 s	Peak spectral period
	U_c	1 m/s	Current velocity
	Φ	5.43	Spreading constant
UWAPIPE	μ_o	0.40	Yield surface shape parameter
	κ	0.65	Gradient of the parameter μ_o with increasing depth
	β	0.06	Yield surface shape parameter
	μ_t	0.65	Plastic potential surface shape parameter
	m	0.18	Aspect ratio of plastic potential surface
	k_{ve}	8000 kN/m/m	Elastic vertical stiffness
	k_{he}	8000 kN/m/m	Elastic horizontal stiffness
	k_{vp}	400 kN/m/m	Plastic vertical stiffness
Pipe	E	2.1E11 kN/m2	Young's modulus
	D	1.0 m	Pipe diameter
	t_s	0.03 m	Pipe thickness
Initial Condition	V_0	10.12 kN/m	Intersection of bounding surface and V axis
	Ws	5.06 kN/m	Pipe self-weight
	H	0 kN/m	Horizontal force

TABLE 2. RESPONSE SURFACE PARAMETERS VALUES

Parameter Type	Number	Response Surface Variables	Mean Value	Standard deviation	COV %
Soil Modeling	1	k_{vp}, Plastic vertical stiffness	400	100	25
	2	μ_o, Yield surface shape parameter	0.4	0.04	10
	3	κ, (μ_o gradient with depth)	0.65	0.13	20
Pipe Modeling	4	EI, Pipe bending stiffness	3.37E06	3.37E05	10
	5	V_0, Load concentration at TDZ	4.2	1.05	25
Hydro-dynamics Modeling	6	d, Water depth	55	1.925	3.5
	7	Lift & Drag forces, Fourier coeff.	----	----	20
	8	Inertial force, coeff.	3.29	0.4935	15

TABLE 3. RESPONSE SURFACE POLYNOMIAL COEFFICIENTS

Xi	a	b_i	c_i	d_{ij} (X_j = …)							
				1	2	3	4	5	6	7	8
1	1.21E+02	2.61E-02	2.65E-06	----	-2.11E-02	6.19E-05	-2.65E-10	1.16E-04	-5.62E-04	1.38E-02	6.31E-04
2	----	-9.82E+01	4.89E+01	----	----	5.05E+00	5.14E-07	3.26E-02	1.71E+00	-3.99E+01	-9.27E-01
3	----	-9.26E+00	2.56E+00	----	----	----	4.49E-08	-8.58E-03	1.02E-01	-2.32E+00	-7.32E-02
4	----	-3.87E-06	3.81E-13	----	----	----	----	5.36E-09	3.30E-08	-8.23E-07	-1.28E-08
5	----	-4.45E-01	3.35E-02	----	----	----	----	----	3.10E-03	-1.24E-01	-8.93E-03
6	----	-4.76E+00	4.92E-02	----	----	----	----	----	----	-1.63E+00	-3.57E-02
7	----	8.62E+01	1.30E+01	----	----	----	----	----	----	----	3.55E-01
8	----	1.55E+00	2.01E-01	----	----	----	----	----	----	----	----

TABLE 4. SENSITIVITY ANALYSIS OF PIPELINE STABILITY VARIABLES

N =10000 $\Delta\mu_{Xi}$= 1%			R = Max. H. Disp. (1 D)			R = Max. H. Disp. (2.5 D)			R = Max. H. Disp. (5 D)			R = Max. H. Disp. (10 D)		
			P_f = 0.4762			P_f =0.2478			P_f =0.0922			P_f =0.0143		
Xi	Type	+/-	Pf (ΔμXi)	SμXi	Rank	Pf (ΔμXi)	SμXi	Rank	Pf (ΔμXi)	SμXi	Rank	Pf (ΔμXi)	SμXi	Rank
1	k_{vp}	+	0.4773	0.11	4	0.2497	0.19	4	0.0934	0.12	4	0.0145	0.02	4
2	μ	-	0.482	0.58	3	0.2538	0.60	3	0.0955	0.33	3	0.0148	0.05	3
3	κ	-	0.4765	0.03	7	0.248	0.02	6-7	0.0924	0.02	6-7	0.0144	0.01	5-6
4	EI	-	0.4769	0.07	5	0.2485	0.07	5	0.0926	0.04	5	0.0144	0.01	5-6
5	V_0	-	0.4766	0.04	6	0.248	0.02	6-7	0.0924	0.02	6-7	0.0143	0.00	7-8
6	d	-	0.5153	3.91	1	0.2824	3.46	1	0.1079	1.57	1	0.0193	0.50	1
7	Fourier coeff.	+	0.4884	1.22	2	0.2623	1.45	2	0.099	0.68	2	0.0161	0.18	2
8	Inertia coeff.	+	0.4764	0.02	8	0.2479	0.01	8	0.0923	0.01	8	0.0143	0.00	7-8